Channel-Dropping Filter Based on a Grating-Frustrated Two-Core Fiber

A.-C. Jacob-Poulin, R. Vallée, S. LaRochelle, D. Faucher, and G. R. Atkins

***Abstract*—We present experimental results on the operation of a dissimilar two-core fiber segment as a channel-dropping filter based on the principle of grating-frustrated coupling. The restoration of 100% coupling by ultraviolet (UV)-tuning of the fiber is demonstrated over a bandwidth in excess of 20 nm. It is also shown that a grating can be inscribed in one of the cores while maintaining perfect coupling conditions between the cores.**

***Index Terms*—Channel-dropping filter, intracore Bragg grating, optical fiber device, two-core fiber, ultraviolet (UV)-tuning.**

I. Introduction

WAVELENGTH-SELECTIVE devices are basic components of optical communications systems based on wavelength-division multiplexing (WDM). Ideally, all-optical elements with low insertion losses, polarization insensitivity and good spectral selectivity are required. Accordingly, all-fiber devices that utilize the well-established technology of intracore Bragg gratings are good candidates for WDM applications. However, a Bragg grating alone operates in reflection mode and is not practical for many applications, and an approach which is increasingly favored is based on the conjoint use of Bragg gratings with directional couplers. Recently, various filters involving both gratings and either fused [1], [2], polished [3], [4] or two-core fiber [5], [6] couplers were proposed. In devices involving two-core fibers, the grating is located outside the coupling region, whereas in the others the grating action occurs within the coupling region.

This paper is based on a two-core fiber device involving a grating located in the middle of the coupling region. Our device relies on the photosensitivity of germanium-doped silica glass, which allows both the writing of a Bragg grating and the control of the coupling conditions by ultraviolet (UV) tuning [7] of the two-core fiber. Its basic principle of operation is based on grating-frustrated coupling, as originally proposed by Archambault *et al.* [3] for a polished-type fiber coupler. A major advantage of the two-core fiber coupler for performing grating-frustrated coupling is that it allows for a longer coupling length, which is a crucial parameter as we show hereafter. In essence, grating-frustrated coupling relies on the dephasing action of a grating that prevents exchange of energy between two otherwise synchronous waveguides in the vicinity of the grating bandgap. Therefore, it is mainly the dispersive rather than the reflective property of the grating that is used here. Note that, in this case, where the two waveguides are synchronous (i.e., their propagation constants are equal), the grating dispersion plays a dephasing role, but it has been demonstrated that it can equivalently play a synchronizing role when the guides are initially asynchronous [8]. This situation should not be confused with grating-assisted coupling that occurs when long-period gratings are used. For a grating-frustrated-coupler to work properly, complete exchange of power must take place between the cores in the vicinity of the Bragg wavelength, which requires the two cores to have closely matched propagation constants. In practice though, it is extremely difficult to fabricate such perfectly-matched two-core fibers, and the UV-induced refractive index modulation forming the intra-core grating is always accompanied by a dc component that detunes the cores anyway. Although coupling between two slightly detuned cores can be locally restored by bending [9], [10], UV tuning is more practical in the present case.

Manuscript received September 15, 1999; revised January 24, 2000. This work was supported by NSERC (National Sciences and Engineering Research Council of Canada).

A.-C. Jacob-Poulin, R. Vallée, S. LaRochelle, and D. Faucher are with the Centre d'optique, photonique et laser, Département de Physique, Université Laval, Sainte-Foy, PQ, G1K7P4, Canada (e-mail: rvallee@phy.ulaval.ca).

G. R. Atkins is with the Optical Fibre Technology Centre, Australian Photonics Cooperative Research Centre, University of Sydney, NSW 2006, Australia (e-mail: g.atkins@oftc.usyd.edu.au).

Publisher Item Identifier S 0733-8724(00)03738-5.

II. Theoretical Model

Fig. 1 is a schematic of the two-core grating frustrated coupler, where core 1 contains a UV-written Bragg grating and core 2 contains a uniformly UV-exposed region. We restrict our analysis to the case where the input field into core 1 is zero. In general, as it propagates along core 2, the input field will be coupled to core 1 while passing through the coupling region ($L_C = \pi/2C$) if its wavelength is sufficiently far from the Bragg wavelength. In the vicinity of the Bragg wavelength, and provided that the grating (i.e., κ) is strong enough, the dephasing action of the grating will prevent coupling to core 1 so that most of the field will remain in core 2. Note that the grating length L_G is deliberately made longer than the coupler length to increase the barrier effect created by the grating. Thus, the grating-frustrated coupler behaves like a channel-dropping filter for an input field into core 2. The evolution of the forward and backward fields propagating in both cores is readily derived on the basis of coupled-mode theory. Letting A_1, B_1, A_2, and B_2 denote the forward and backward fields into core 1 and 2, respectively, and κ and C the grating and coupler coupling constants respectively, one has over the coupling region

$$A_2' = iCA_1 \exp(i\Delta\beta z) \tag{1a}$$

$$B_2' = iCB_1 \exp(i\Delta\beta z) \tag{1b}$$

$$A_1' = iCA_2 \exp(-i\Delta\beta z) + i\kappa B_1 \exp(-2i\delta z) \tag{1c}$$

$$B_1' = iCB_2 \exp(-i\Delta\beta z) - i\kappa A_1 \exp(2i\delta z) \tag{1d}$$

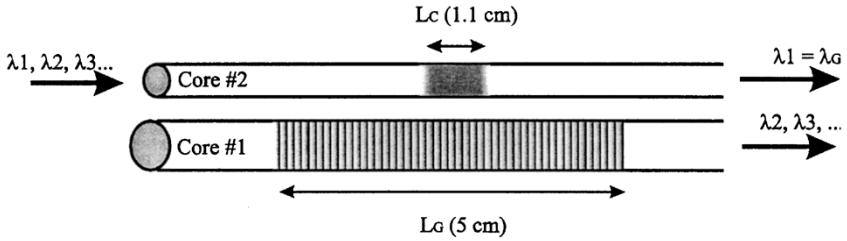

Fig. 1. Schematic of the two-core grating-frustrated coupler.

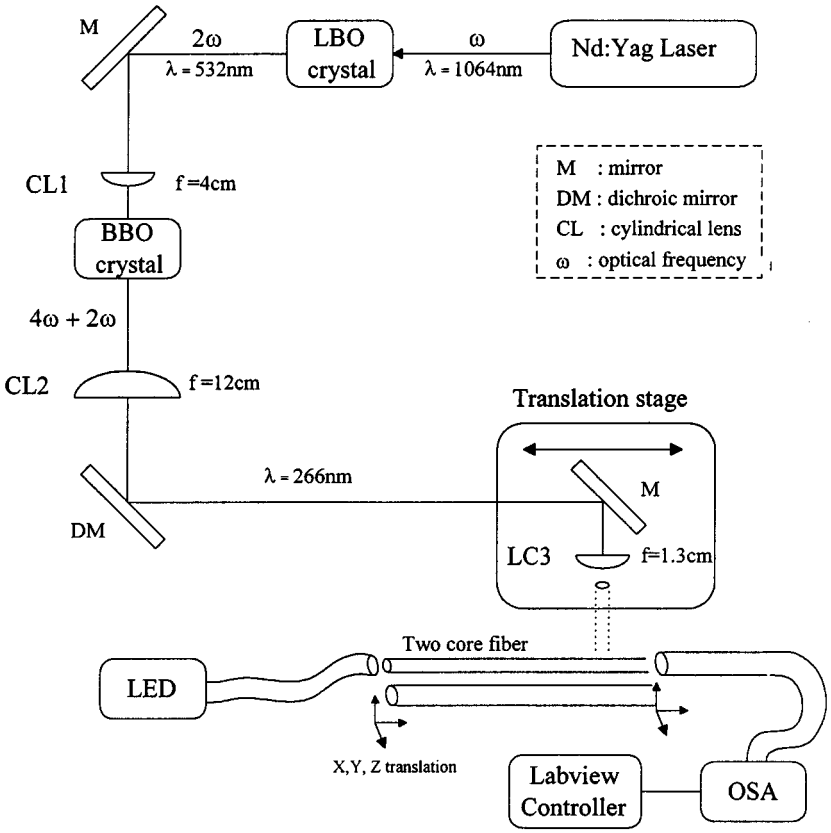

Fig. 2. Experimental setup.

where the prime $(')$ indicates differentiation with respect to z. The coupler and grating detuning parameters are, respectively

$$\Delta\beta = \beta_1 - \beta_2 \tag{2a}$$

$$\delta = \frac{\beta_1 + \beta_2 - K}{2} \tag{2b}$$

with

$$K = \frac{2\pi}{\Lambda} \quad (\Lambda = \text{grating period}). \tag{3}$$

A simplification of the set of coupled equations (1) can be made by assuming (in agreement with the experimental results) that the two cores are perfectly phase-matched (i.e., $\Delta\beta = 0$) in the vicinity of the Bragg wavelength. The resulting set of equations, along with its boundary conditions, can be solved analytically. In core 1, the fields are further subject to continuity conditions with fields propagating in the two segments (on either side) where the grating extends beyond the coupling region. In these two regions, A_1 and B_1 are simply related by the coupled-wave equations for a uniform grating.

III. Experiment

The experimental setup is shown in Fig. 2. A UV beam at 266 nm, obtained from a frequency quadrupled CW-mode-locked Nd-YAG laser, was used to produce the refractive index changes in the fiber cores. A crucial requirement was to obtain an aberration-free UV spot so that one could selectively illuminate one core at a time. Careful adjustment of the doubling crystals and of the cylindrical lenses allowed us to produce an elliptical focal spot of ~ 7 μm (transversally) by ~ 500 μm (along the fiber axis). A precision translation stage allowed the focussed beam to be translated a few centimeters along the exposed core without significant transverse shift. By careful examination of the blue fluorescence pattern exiting the fiber, we ensured that only one core was exposed at a time.

The dissimilar two-core fiber was fabricated at the Optical Fibre Technology Centre of the University of Sydney. The two-core preform was assembled by machining pieces of two different single-core preforms into D-sections and fusing them together. Accordingly, the two cores are roughly lying

TABLE I

		Core #1	Core #2
Core radii (μm)		3.7	2.4
Separation center to center (μm)		17.0	
Numerical aperture (NA)		0.118	0.126
Dopant level (% mol)	GeO_2	3.2 ± 0.2	5.2 ± 0.1
	P_2O_5	0.6 ± 0.1	0
	B_2O_3	0	4.4 ± 0.2
Refractive index (@1550nm)		1.44886	1.44948
Effective index (@1550nm)		1.44565	1.44460
Relative detuning: $\Delta\beta/\beta$		7.3×10^{-4}	
Theoretical coupling length (mm)		9.4	

symmetrically about the fiber axis. The main characteristics of this fiber are summarized in Table I, with the geometrical parameters (core radii and center to center core separation) measured with a *York S200 Video Fiber Analyzer*. Since precise knowledge of the fiber parameters is essential to determine accurately the coupling parameters, careful measurements of the concentration profiles of core 1 (phosphorus co-doped germanosilicate) and core 2 (boron codoped germanosilicate) were made with an electron microprobe (Cameca SX-100). From these profiles (shown in Fig. 3) we inferred the corresponding molar percentages of the constituents and therefore the refractive indexes of both cores via Sellmeier relations. The cladding was pure silica, since neither of the single-core preforms had a deposited cladding. We were expecting core 1 to be less photosensitive than core 2 (confirmed experimentally), and hydrogen loading proved necessary to produce refractive index variations on the order of 10^{-3}. Note that in our calculations, we assumed that the phosphorus content of core 1 was so low that its effect on the refractive index, compared to the effect of the germanium, could be neglected.

The first part of the experiment consisted in establishing the appropriate conditions for restoring coupling between the cores in the vicinity of 1550 nm. For this purpose, preliminary tests were required to determine precisely the coupling length L_C of the two-core fiber sample. By moving the focussed UV beam several times over segments of various lengths, we established that the optimum value for L_C was 11 mm. During this process, light from a broadband light-emitting diode (LED) was launched into core 2, and the output from this core was directed to an optical spectrum analyzer (OSA) via a butt-coupled fiber to monitor the wavelength response of the coupler. Both the translation stage and the OSA were controlled by LabVIEW to enable real-time monitoring of the fiber transmission. In this manner, the evolution of the coupling as a function of UV exposure could be monitored, and the exposure interrupted the moment 100% coupling was restored over the required wavelength range. Note that it was necessary to make the center of the coupling region coincide with the Bragg wavelength. A typical spectrum of the resulting

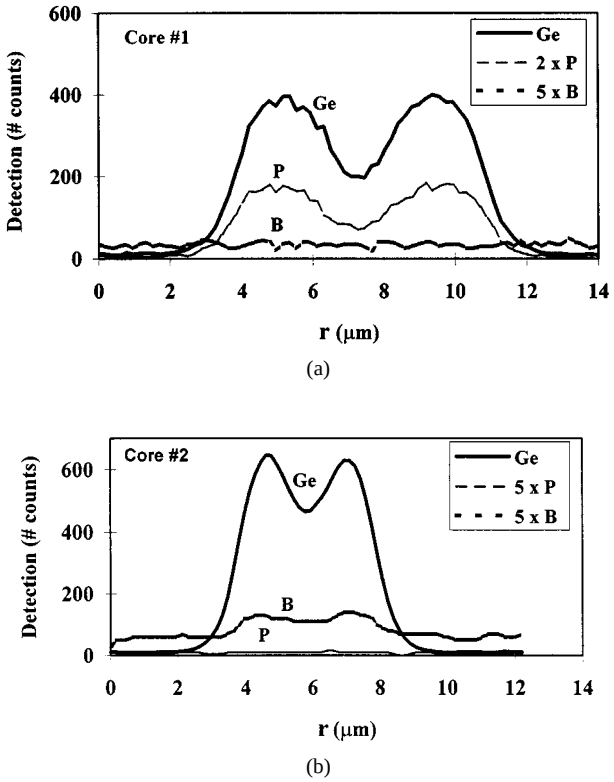

Fig. 3. Concentration profiles of the various constituents of the two cores, with vertical axes given in terms of detected counts. Calibration curves from known standards for each element were used to convert the data to molar concentrations. The origin of r is arbitrary (i.e., it does not correspond to the fiber axis). Note that there is not a linear relationship between the #counts and the %mol of the various constituents.

UV-restored coupler is shown in Fig. 4(a), where the outputs of the two cores are plotted, along with their sum, on a log scale. A coupling ratio in excess of 25 dB is observed over a wavelength range of 20 nm centered at 1550 nm. On a linear scale [Fig. 4(b)], the coupling region appears as a 20 nm wide plateau where practically 100% energy transfer occurs from core 2 to core 1. The signal-to-noise ratio (SNR) is degraded on either side of the coupling region because the transmitted LED power decreased below the noise detection floor, and the oscillations occurring near 1590 nm are related to the detection procedure rather than the coupling device itself.

In the second part of the experiment, a two-core fiber grating-frustrated coupler was fabricated. In the first step, a strong Bragg grating was written into core 1 by translating a 130-mW, 7×500 μm^2 UV spot once along a 5-cm-long phase mask (in close proximity to the fiber) at 10 mm/min. The resulting Bragg grating, centered at 1554.06 nm, had a bandwidth of 0.7 nm and a power reflectivity in excess of 20 dB. In the second step, the phase mask was removed and core 2 was exposed to the UV beam over a length corresponding precisely to the previously measured coupling length (11 mm) to compensate for both the intrinsic and the UV-induced (by the grating writing) phase mismatch between the two cores. In this second step, the same UV intensity and translation speed were used, but the beam was now translated five times over the 11-mm-long segment located at the middle of the 5 cm long grating region (see Fig. 1). In this manner, perfect restoration of coupling could be obtained around 1550 nm, but now

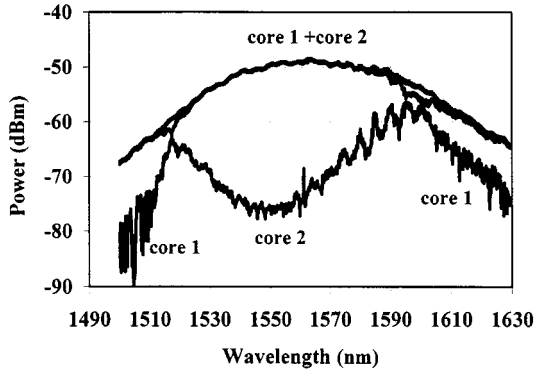

(a)

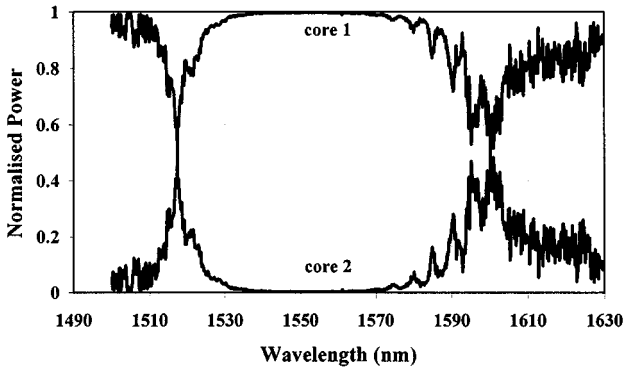

(b)

Fig. 4. (a) Log plots of the outputs of the two cores, and their sum, as a function of wavelength, after UV-induced restoration of coupling. (b) Same outputs on a normalized linear scale.

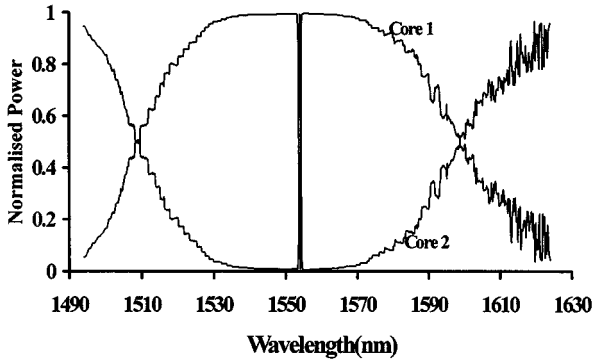

(a)

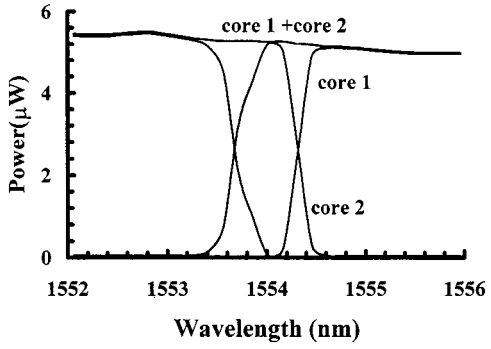

(b)

Fig. 5. (a) Normalized output powers of cores 1 and 2 in the grating-frustrated coupler configuration. (b) Expansion of the Bragg wavelength region, with powers expressed in absolute value (μW) and the sampling points (spaced by 0.15 nm) linked using a spline function.

accompanied by a central dip corresponding to the presence of the grating, as shown in Fig. 5(a). For this measurement, light from the LED was launched into core 2 and the output from each core was sent alternately (via a single-mode fiber patchcord) to the OSA. Special attention was paid to ensure that the light from each core be well separated. From Fig. 5(a), we observe that directional coupling is restored over a 90-nm region (FWHM) centered at 1555 nm. We also note that the two curves are symmetrical with each other and that their sum is nearly constant, showing that energy exchange between the two cores is not significantly perturbed by loss mechanisms, at least up to 1610 nm. From an expansion of the central dip shown in Fig. 5(b), we can estimate that the grating bandwidth (FWHM) remained on the order of 0.7 nm, i.e., essentially unaltered by the UV-trimming process. (Note that the resolution of the spectrum was limited by the OSA sampling spacing of 0.15 nm.) Accordingly, we stress that during the UV-trimming process, we could observe that light was progressively transferred from core 2 to core 1 over the whole coupling band except at the Bragg wavelength, for which light always remained in core 2. This illustrates that coupling from core 2 to core 1 was indeed frustrated at the Bragg wavelength by the presence of the grating in core 1.

IV. Discussion

A. UV-Tuned Two-Core Fiber

In restoring coupling in the dissimilar TCF that we used, it is important to recall that it had a relatively large intrinsic detuning (7×10^{-4}, see Table I). The refractive index change Δn_2 (in core 2) necessary to compensate for this detuning was $\approx 2.5 \times 10^{-3}$, and cannot be regarded as a slight perturbation to the guiding structure. Such an increase significantly affects the confinement factor of the mode propagating in this core, so that the UV-induced Δn_2 results not only in a change in the propagation constant β_2, but also in the coupling coefficient C. (We verified this by performing an exhaustive numerical simulation (BPM) of the coupler as well as direct calculations of the overlap integrals of the fields, before and after UV tuning.) One must, therefore, keep in mind that UV irradiation affects simultaneously the two conditions for 100% coupling: $\Delta\beta = 0$ and $C.L = \pi/2$. Accordingly, in the process of restoring coupling between the cores, the general trend we observed (illustrated in Fig. 6) was for the maximum coupling wavelength, as well as the maximum itself, to increase with UV irradiation of the smaller core (core 2). Now, the shift of the coupling maximum toward longer wavelengths can be understood by noting that, since waveguide dispersion is larger in the smaller core, one has $|d\beta_2/d\lambda| > |d\beta_1/d\lambda|$ so that increasing β_2 (through Δn_2) results in a shift of the tuning wavelength (where $\beta_1 = \beta_2$) toward longer wavelengths. As for the increase in the maximum coupling ratio, it is directly related to the fact that the condition $C.L = \pi/2$ actually implies that $L = L_C$, with L (the coupler length) equal to a constant (11 mm) and L_C (the coupling length) generally decreasing with increasing wavelength. Thus, one has initially a situation such that $L_C > L$, but as

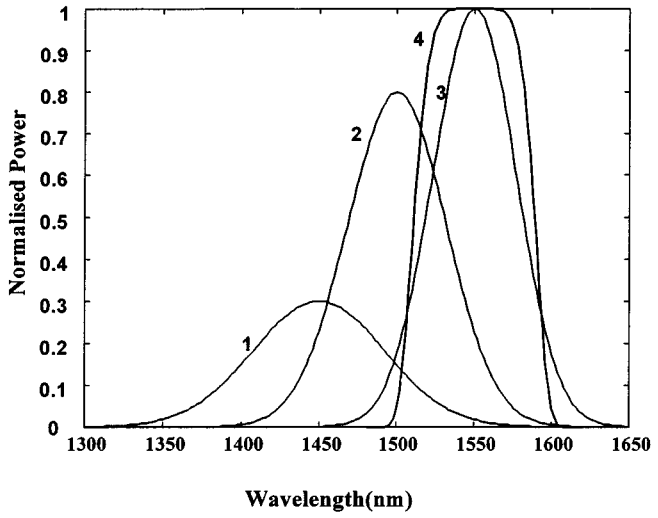

Fig. 6. Schematic representation of the typical evolution of the spectral transfer function of a UV-tuned coupler as a function of the UV exposure. The numbers associated with each curve represent (nominally) the number of passes of the UV spot on a given fiber segment.

Δn_2 (and therefore $\Delta\beta_2$) is increased, the tuning wavelength is also increased, so that L_C is decreasing and is therefore getting closer to L. One eventually reaches 100% coupling when L_C is becoming equal to L, which occurs at 1550 nm. Note that, initially, one had to determine experimentally the appropriate coupler length such that 100% coupling is restored precisely at 1550 nm. The experimental value of 11 mm is in good agreement with the theoretical value computed using the formulas for dissimilar cores derived by Snyder and Ankiewicz [11], considering that the theoretical value for the quantity $\pi/2C$ increases from 9.4 to 14.7 mm when the refractive index of core 2 is increased from its original value of 1.4495 to its UV-modified value of 1.4520 (@ 1550 nm). Note that it is not particularly relevant to speak in terms of the effective coupling length (i.e., $\pi F/2C$) in the mismatched case, because the transfer factor F is then very close to zero. In fact, the crucial parameter here is the coupling constant C, since it is directly related to the overlap integral of the fields.

If the UV irradiation were further continued such that L_C became smaller than L, one might expect that overcoupling would occur. Instead, we observed that the coupling peak tended, for a while, to widen so as to form the extended region or plateau over which 100% coupling was maintained (see Figs. 4 and 5). Eventually, however, the plateau disappeared with further UV irradiation, so that the maximum coupling would rapidly decrease from 100% while continuing to shift toward longer wavelengths. We checked that it was possible to "recompensate" for the induced mismatch (with β_2 now larger than β_1) by irradiating core 1, but the tuning wavelength continued to shift toward longer wavelengths.

The first comment that can be made about this plateau behavior is that it cannot be understood on the basis of the standard coupled-mode equations (with constant parameters), which predict that complete energy exchange occurs only at the tuning wavelength, i.e., where $\beta_1 = \beta_2$. While intriguing, this phenomenon is also fortunate, as a coupler with spectral properties characterized by an extended coupling zone and a sharp transition between high and low crossover values is likely to find interesting applications. Such behavior is typical of couplers having length equal to odd integer multiples of $\pi/2C$ [12], but based on the previous discussion on the typical behavior our device (Fig. 6), this possibility must be excluded. It was also shown by Hewlett *et al.* [13] that couplers with very broad transfer functions could be obtained by taking advantage of the spectral dependence of the coupling coefficients. Specifically, a quartic behavior can be obtained when the coupling wavelength is made coincident with the turning point of the coupling coefficient ($dC/d\lambda = 0$). However, this hypothesis must also be excluded in our case since $dC/d\lambda$ is still quite large ($\approx 0.5\ \text{mm}^{-1}\cdot\mu\text{m}^{-1}$) at 1.55 μm. A third possibility is that, for some reason, the irradiation pattern was not perfectly uniform along the fiber (z). In fact, although careful attention was paid to align the translation of the focussed beam with the fiber core to be exposed, the possibility that some deviation occurred cannot be ruled out. It is also possible that the focussed beam might not have been perfectly uniform transversally. In either case, both C and $\Delta\beta$ could have acquired a functional dependence on z. According to Alferness and Cross [14] the spectral transmission of a coupler can be significantly altered by a taper function on either C or $\Delta\beta$. It was also shown that, in general, the Fourier transform of the taper function $C(z)$ shared some similarity with the spectral response of the device. On that basis, the most likely taper function which would explain the obtained rectangle-like spectral transmission is a sinc-like function, and numerical simulations are in progress to test the likeliness of this hypothesis.

B. Grating-Frustrated Coupler

Because grating-frustrated coupling relies on the phase mismatch induced by a grating, the coupling and grating parameters must be chosen carefully to establish good working conditions. A basic requirement is that the grating constant κ be large in comparison to the coupling coefficient C. This ensures that the grating dephasing action occurs before the coupling process builds up. The relative strength between the grating and the coupler is conveniently quantified by the product $\kappa \cdot L_C$, and the major advantage of the two-core fiber is that it allows both κ and L_C to take larger values than are readily obtainable in a polished-type coupler. To estimate $\kappa \cdot L_C$ for our device, the effective or mode index modulation δn can be computed from the formula valid for strong gratings: $\Delta\lambda = \lambda_B \delta n / n_{\text{eff}}$. From the measured value of $\Delta\lambda$ (0.7 nm) one gets $\delta n = 7 \times 10^{-4}$, and from $\kappa = \pi\delta n/\lambda$ one obtains $\kappa = 1.4\ \text{mm}^{-1}$. Thus, recalling that $L_C = 11$ mm, one obtains $\kappa \cdot L_C \approx 15$ which, according to the theoretical analysis, lies in the ideal range for operation of the device as a channel-dropping filter. Indeed, within this range, both reflection coefficients are tending to zero so that the frustrated coupler behaves truly like a transmission device (Fig. 7). It is precisely under these conditions that our device was operating, so that a negligible amount of signal was reflected. In terms of transmissions, we measured an isolation of 22 dB of the signal at the Bragg wavelength exiting core 2, whereas 20 dB extinction of this signal was observed at the core 1 output. The bandwidth of the transmission notch was 0.7 nm (equal to the bandwidth of the grating alone), a somewhat surprising result since, according to the theoretical analysis, the frustrated-coupler bandwidth should get wider for larger values of the product $\kappa \cdot L_C$. The most likely explanation for this would rely on the

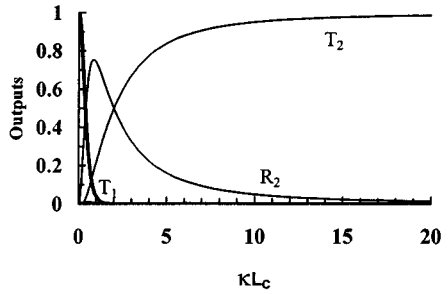

Fig. 7. Theoretical outputs of the grating-frustrated coupler as a function of κL_C at the Bragg wavelength (computed from eqs 1 with $\Delta\beta = 0$). T_2 and R_2 refer to the normalized transmission and reflection from core 2 respectively, whereas T_1 is the transmission from core 1. The reflection from core 1, R_1, is negligible on this scale.

previously discussed hypothesis that the coupling coefficient is z-dependent. Numerical simulations will be required to verify this hypothesis because the system of (1) has, in general, no analytical solution for a z-dependent C (or $\Delta\beta$).

A final comment should be made concerning the ageing of our device. We observed that over a period of hours following the UV processing, the performance of the frustrated coupler tended to degrade, partially in some cases, but more dramatically in others. Typically there was a progressive shift of the coupling region toward longer wavelengths accompanied by a reduction of the maximum coupling ratio from 100% to 50–70%, and even lower in some cases. A correlation was established between the number of days of hydrogen soaking and the degree of degradation of the coupler, and ideally the hydrogen soaking process should be avoided if stable devices are to be produced. Hydrogen soaking could not be avoided in this experiment, because the TCF sample had an excessively large intrinsic detuning. By using a more efficient writing wavelength (e.g., 193 or 244 nm) and a TCF sample with a smaller intrinsic detuning, stable and reliable two-core grating-frustrated couplers could readily be produced.

V. Conclusion

We have shown that a narrow channel-dropping filter can be produced based on a grating-frustrated two-core fiber (TCF). Specifically, we demonstrated that a Bragg grating can be inscribed in one core of the TCF while restoring and maintaining 100% coupling by UV-tuning over a given segment. The coupling spectrum appeared to take a peculiar form characterized by a plateau where almost 100% power transfer occurred, possibly related to a nonuniform illumination of the fiber core. Although requiring further investigation, this flat-topped response is advantageous for WDM applications, and the UV trimming technique may be further refined by deliberately modifying the relative detuning or the coupling coefficient as a function of z, so as to tailor the spectral response of the coupler. The main difficulty of our device is its poor ageing stability, which is related directly to the necessity to sensitize the fiber by hydrogen loading. This problem could be readily overcome by using a TCF sample with a smaller intrinsic detuning and, ideally, a more efficient writing wavelength than 266 nm. Finally, further tests should be performed in order to verify the long-term stability as well as the polarization dependence of the device, which have not been addressed in this work.

Acknowledgment

The authors would like to acknowledge Prof. J. D. Love for helpful discussions and P. Grenier, E. Tremblay, and P.-Y. Cortès for their technical assistance.

References

[1] F. Bakhti, P. Sansonetti, C. Sinet, L. Gasca, L. Martineau, S. Lacroix, X. Daxhelet, and F. Gonthier, "Optical add/drop multiplexer based on UV-written Bragg grating in a fused 100% coupler," *Electron. Lett.*, vol. 33, pp. 803–804, Apr. 1997.

[2] A. S. Kewitsch, G. A. Rakuljic, P. A. Willems, and A. Yariv, "All-fiber zero-insertion-loss add-drop filter for wavelength-division multiplexing," *Opt. Lett.*, vol. 23, pp. 106–109, Jan. 1998.

[3] J.-L. Archambault, P. St. J. Russell, S. Barcelos, P. Hua, and L. Reekie, "Grating-frustrated coupler: A novel channel-dropping filter in single-mode optical fiber," *Opt. Lett.*, vol. 19, pp. 180–183, Feb. 1994.

[4] I. Baumann, J. Seifert, and M. Sauer, "Compact all-fiber add-drop-multiplexer using fiber Bragg gratings," *IEEE Photon. Technol. Lett.*, vol. 8, pp. 1331–1333, Oct. 1996.

[5] S. Bethuys, L. Lablonde, L. Rivoallan, J. F. Bayon, L. Brilland, and E. Delevaque, "Optical add/drop multiplexer based on UV-written Bragg gratings in twincore fiber Mach–Zehnder interferometer," *Electron. Lett.*, vol. 34, pp. 1250–1253, June 1998.

[6] B. O. Ortega, L. Dong, and L. Reekie, "All-fiber optical add-drop multiplexer based on a selective fused coupler and a single fiber Bragg grating," *Appl. Opt.*, vol. 37, pp. 7712–7717, Nov. 1998.

[7] G. R. Atkins, J. W. Arkwright, and S. J. Hewlett, "UV tuning of coupling in twin-core optical cores," *Electron. Lett.*, vol. 30, no. 25, pp. 2165–2166, Dec. 1994.

[8] A. Ankiewicz, Z. H. Wang, and G. D. Peng, "Analysis of narrow bandpass filter using coupler with Bragg grating in transmission," *Opt. Commun.*, vol. 156, pp. 27–31, Nov. 1998.

[9] R. Vallée and D. Drolet, "Practical coupling device based on a two-core optical fiber," *Appl. Opt.*, vol. 33, pp. 5602–5610, Aug. 1994.

[10] J. W. Arkwright, S. J. Hewlett, G. R. Atkins, and B. Wu, "High-isolation demultiplexing in bend-tuned twin-core fiber," *J. Lightwave Technol.*, vol. 14, pp. 1740–1745, July 1996.

[11] A. W. Snyder and A. Ankiewicz, "Optimal fiber couplers-optimum solution for unequal cores," *J. Lightwave Technol.*, vol. 6, pp. 463–474, Mar. 1988.

[12] D. Marcuse, "Bandwidth of forward and backward coupling directional couplers," *J. Lightwave Technol.*, vol. LT-5, pp. 1773–1777, Dec. 1987.

[13] S. J. Hewlett, J. D. Love, and V. V. Steblina, "Analysis and design of highly broad-band planar evanescent couplers," *Optic. Quantum Electron.*, vol. 28, pp. 71–81, 1996.

[14] R. C. Alferness and P. Cross, "Filter characteristics of codirectionally coupled waveguides with weighted coupling," *IEEE J. Quantum Electron.*, vol. QE-14, pp. 843–847, Nov. 1978.

A.-C. Jacob-Poulin, photograph and biography not available at the time of publication.

R. Vallée, photograph and biography not available at the time of publication.

S. LaRochelle, photograph and biography not available at the time of publication.

D. Faucher, photograph and biography not available at the time of publication.

G. R. Atkins, photograph and biography not available at the time of publication.